ELSEVIER
Journal of Materials Processing Technology 108 (2001) 193–196
Journal of Materials Processing Technology
www.elsevier.com/locate/jmatprotec

Pulsed laser deposition of mixed valence manganite artificial superstructures

I. Panagiotopoulos[a,*], C. Christides[b], M. Pissas[a], D. Niarchos[a]

[a]Institute of Materials Science, NCSR Demokritos, Ag. Paraskevi Attiki, 15310 Athens, Greece
[b]Department of Engineering Sciences, School of Engineering, University of Patras, 26110 Patras, Greece

Abstract

The magnetic structural and magnetotransport properties are studied in a series of $[La_{2/3}Ca_{1/3}MnO_3/La_{1/3}Ca_{2/3}MnO_3]_{15}$ multilayers prepared by pulsed laser deposition. The $La_{2/3}Ca_{1/3}MnO_3$ layers are ferromagnetic (FM) and $La_{1/3}Ca_{1/3}MnO_3$ layers are antiferromagnetic (AF). The structural compatibility of the AF and FM layers permits coherent growth that favors magnetic coupling. The hysteresis loops of field cooled samples are shifted. This is attributed to the presence of an exchange biasing mechanism at low temperatures. Zero-field-cooling and field-cooling magnetic measurements reveal a blocking temperature around 70 K that is independent from the bilayer thickness, whereas the average film magnetization becomes zero at 250 K.

Keywords: Pulsed laser deposition; Exchange biasing; Multilayers; Mixed valance manganites

1. Introduction

Despite the extensive study of the so-called Colossal magnetoresistance (CMR) manganese perovskites [1] little progress has been made towards using these materials in applications. This is mainly due to the strong temperature dependence and the large saturation fields (of the order of Tesla) of the CMR effect.

In order to deal with this problem different approaches have been considered as the magneto-tunneling effect in CMR/Insulator/CMR trilayer epitaxial junctions [2,3] and the effect of grain boundary scattering giving rise to a "GMR-like" mechanism of magnetoresistance (MR) [4–7].

The preparation of artificial superstructures is another route to optimize the CMR behavior and understand the mechanisms involved in this phenomenon [8–11]. The properties of such structures are not a mere superposition of the response of the individual layers. This could be attributed to either interlayer interactions or stress effects due to lattice mismatch [11]. In what follows we report on the magnetic structural and MR properties of $La_{2/3}Ca_{1/3}MnO_3/La_{1/3}Ca_{2/3}MnO_3$ multilayers showing exchange biasing effects. The $La_{2/3}Ca_{1/3}MnO_3$ layers are ferromagnetic (FM) and $La_{1/3}Ca_{1/3}MnO_3$ layers are antiferromagnetic (AF) [1].

The existence of unidirectional anisotropy due to exchange coupling between an FM and an AF phase was first reported in oxide-coated fine particles [12,28] of Co. The exchange anisotropy results in a displaced magnetic hysteresis loop when the sample is field cooled through the Neel temperature of the AF phase. In early studies, this loop displacement has been explained by assuming an ideal FM/AF interface with uncompensated moments in the atomic-plane of the AF layer at the FM/AF boundary [12,28]. Up-to-date exchange anisotropy effects have been studied mainly in AF/FM systems consisting of transition metal alloys and metallic oxides (e.g. FM = Co, NiFe, Fe_3O_4, and AF = CoO, FeMn) [12–19,28,29] but not in manganites, where the magnetic interactions cannot be described by direct exchange.

2. Experimental details

The films were deposited on (0 0 1) $LaAlO_3$ substrates by pulsed laser deposition (PLD) from bulk stoichiometric $La_{2/3}Ca_{1/3}MnO_3$ target samples. The targets were prepared by standard solid state reaction from La_2O_3, $CaCO_3$ and MnO_2 powders sintered at 1300°C for 5 days with two intermediate grindings. MR measurements were performed with a four-probe method and with the current parallel to the applied magnetic field. The θ–2θ X-ray diffraction data were obtained with a Siemens D500 diffractometer using Cu Kα radiation and a secondary graphite monochromator. The

*Corresponding author. Tel.: +30-1-650-3318.
E-mail address: panagiot@ims.demokritos.gr (I. Panagiotopoulos).

0924-0136/01/$ – see front matter
PII: S0924-0136(00)00752-4

magnetic measurements were performed in a SQUID magnetometer (Quantum Design). A series of $La_{2/3}Ca_{1/3}MnO_3/La_{1/3}Ca_{2/3}MnO_3$ multilayers with equal AF and FM layer thickness and bilayer thickness ranging from 2 to 32 nm were grown along the (0 0 1) direction of the simple pseudocubic perovskite unit cell. The structural compatibility of the AF and FM layers permits coherent growth that favors magnetic coupling. In order to deposit in a multilayer form, the targets were mounted on a step-motor controlled rotatable carrier that allows the $La_{2/3}Ca_{1/3}MnO_3$ and $La_{1/3}Ca_{2/3}MnO_3$ targets to be sequentially exposed in the beam path. The substrate was located at a distance of 6 cm from the target, by the edge of the visible extent of the plume. The substrate temperature (T_s) was 700°C and the oxygen pressure in the chamber during the deposition was 0.03 torr. The resulting rate at fluence of 1.5 J/cm^2 on the target was 0.4 Å/pulse.

3. Structural characterization

The existence of the superstructure has been confirmed from the presence of low-angle superlattice Bragg-peaks and multiple satellite peaks around the (0 0 1), (0 0 2) and (0 0 3) Bragg-reflections of the constituents. The main Bragg peak lies between the Bragg peaks observed in single AF and FM layer films and is surrounded by satellite peaks due to the layered structure (Fig. 1). The existence of an average Bragg peak for $\Lambda \leq 10$ nm indicates that for this range of bilayer thickness we have a coherent layer growth. The values of Λ were estimated by the formula $\Lambda = n\lambda_{Cu}/2(\sin\theta_n - \sin\theta_0)$, where θ_n are diffraction angles of the nth order satellite and θ_0 is the average Bragg peak The $(0\,0\,\ell)$ LAO Bragg-peaks ($\ell = 1, 2,$ and 3) interfere with the satellite peaks nearby the fundamental (zeroth order) peaks of the multilayer, introducing uncertainties in the quantitative analysis of the XRD spectra. Asymmetric intensity of the satellite peaks has been reported in multilayers [20,21] in which a chemical and/or strained interfacial profile is assumed along the growth direction of the superlattice. Since for all the examined Λ values there are no traces of mixed (0 0 1) and (1 1 0) textures, cumulative roughness effects resulting to extra surface roughness and mosaic spread [22] with increasing Λ can be excluded.

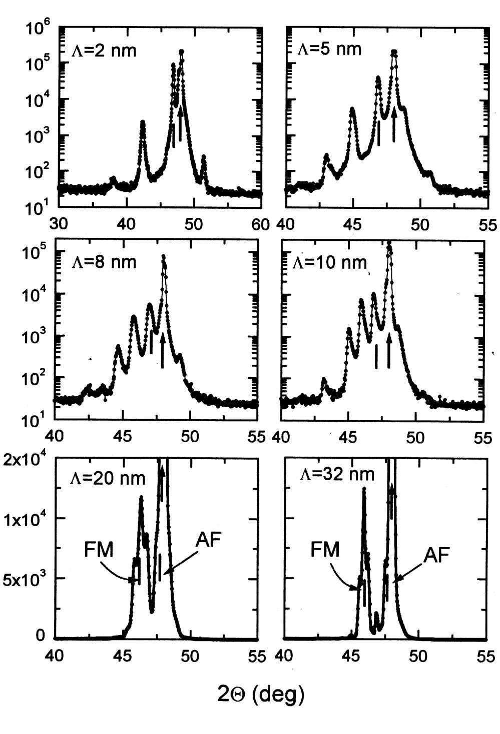

Fig. 1. XRD profiles around the (0 0 2) reflection as a function of bilayer thickness Λ. Arrows indicate the (0 0 2) LAO peak and tick marks show the $n = 0$ (fundamental) peak for $\Lambda < 20$ nm, whereas for $\Lambda = 20$ and 32 nm, the ticks show peaks located at the (0 0 2) reflection of the FM and AF layer.

4. Magnetization and magnetoresistance measurements

Magnetic hysteresis loops, measured at 10 K after cooling down from 300 K in zero field (ZFC) and in 10 kOe (FC), for a $LaAlO_3$/[FM(5 nm)/AF(5 nm)]$_{15}$ sample are shown in Fig. 2. It is evident that the ZFC loop is symmetric around the zero field, while the FC loop is shifted towards negative fields. This effect can be attributed to exchange biasing at the AF/FM interface, since single-layered FM films do not exhibit any loop displacement after the FC process. If H_1 is the lower and H_2 is the higher field value, where the average film magnetization becomes zero, then the exchange biasing field is defined as the loop shift $H_{EB} = -\frac{1}{2}(H_1 + H_2)$ and the coercivity as the halfwidth of the loop $H_C = \frac{1}{2}(H_1 - H_2)$. Thus, we calculate for the FC loop an $H_{EB} = 880$ Oe and an $H_C = 800$ Oe which is almost double compared to the H_C value obtained from the ZFC loop. Additional magnetic measurements were performed in order to investigate the origin of this effect. The temperature dependence of H_{EB} and H_C values is shown in Fig. 3. These values were estimated from isothermal loops measured in constant temperature intervals, after FC the sample from

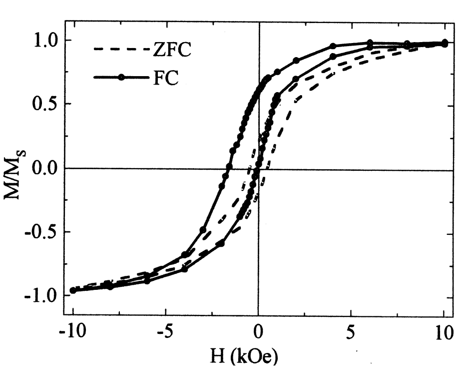

Fig. 2. Hysteresis loops, measured at 10 K after cooling down from 300 K in zero field (ZFC) and in 10 kOe (FC), for a [FM(5 nm)/AF(5 nm)]$_{15}$ multilayer.

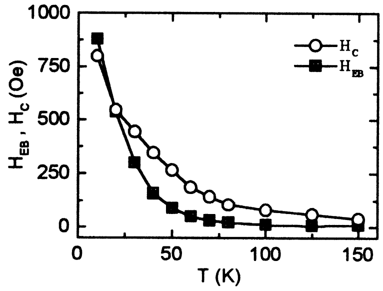

Fig. 3. Temperature dependence of exchange biasing field (H_{EB}) and coercive field (H_C).

300 K down to 10 K in 10 kOe and then warming up. It is evident that H_{EB} decreases and disappears around the so-called blocking temperature T_B of 70 K. The H_C values exhibit a similar trend, indicating a connection between the mechanisms that give rise to coercivity and loop displacement. The excess coercivity observed below T_B is induced by random exchange fields at the AF/FM interfaces. This low-temperature anisotropy can be treated as an additional energy barrier in the magnetic free energy, as in the case of superparamagnetic particles [23].

Since exchange biasing is an interface related phenomenon a strong dependence on the individual FM and AF layer thickness is expected. In order to study the layer thickness dependence of H_{EB} one should try to vary the FM layer thickness keeping the AF layer fixed and vice versa. H_{EB} is reported to have a $1/t_{FM}$ dependence, whereas it is found to be relatively independent of t_{AF} given that it exceeds a certain threshold [14]. However, if the relative AF and FM layer thickness are varied independently there is a change in the average a_p and the resulting structural changes obscure the study of such effects. The observed H_{EB} and H_C values at 10 K, are plotted in Fig. 4 as a function of the bilayer thickness Λ for a series of multilayers with equal AF and FM layer thicknesses $[FM(\Lambda/2)/AF(\Lambda/2)]_{15}$. A maximum H_{EB} is observed for the sample with $\Lambda = 10\,nm$. H_C follows the variation of H_{EB} with Λ, indicating that there is a significant contribution in H_C from the exchange anisotropy at the AF/FM interfaces. The decrease of H_{EB} at higher Λ values as expected due to the decreased contribution of the interfaces. However, H_{EB} also decreases at lower Λ values due to the decreased contribution of the AF layers.

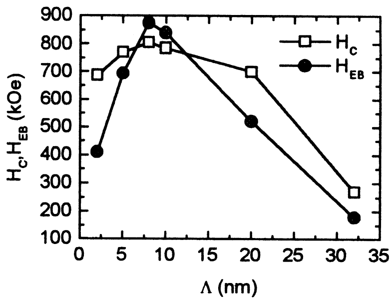

Fig. 4. Exchange biasing field (H_{EB}) and coercive field (H_C) as a function of the bilayer thickness Λ for the series $[FM(\Lambda/2)/AF(\Lambda/2)]_{15}$ of multilayers.

Additional magnetic measurements were performed in order to investigate the origin of this effect. In Fig. 4 the ZFC and FC measurements of the magnetization, normalized to the total FM volume of the sample, are shown for the above series of multilayers as a function of temperature. Both measurements were performed by warming up in 1 kOe after having cooled in zero field and 10 kOe, respectively. The ZFC and FC curves coincide at temperatures higher than 100 K and become zero at about 250 K, where the Curie point T_C of the FM layers is expected. The ZFC curve exhibits a broad peak around the T_B 70 K, whereas the FC curve exhibits a steep increase just below T_B. It is reasonable to assume that in the FC measurement an increase of magnetization results from the alignment of interfacial magnetic moments, giving rise to unidirectional anisotropy [16] below T_B. Hence, the observed hump below T_B in the ZFC curve can be attributed to thermally activated magnetic rotation over energy barriers caused by random exchange coupling at the AF/FM interfaces. Our magnetothermal measurements indicate that the T_B does not change in the examined range of bilayer thickness and occurs at 70 K for all samples. To answer why T_B remains more or less the same in the examined range of Λ values it is reasonable to consider that interfacial spin ordering is confined within a

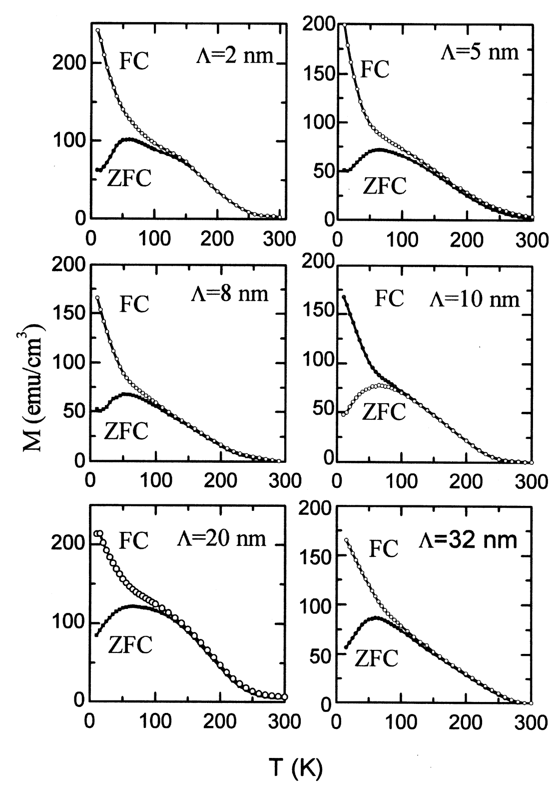

Fig. 5. Magnetization as a function of temperature for the series of $[FM(\Lambda/2\ nm)/AF(\Lambda/2\ nm)]_{15}$ multilayers. The measurements were performed by warming up in 1 kOe after having cooled down to 10 K, in zero field (ZFC) and 10 kOe (FC), respectively.

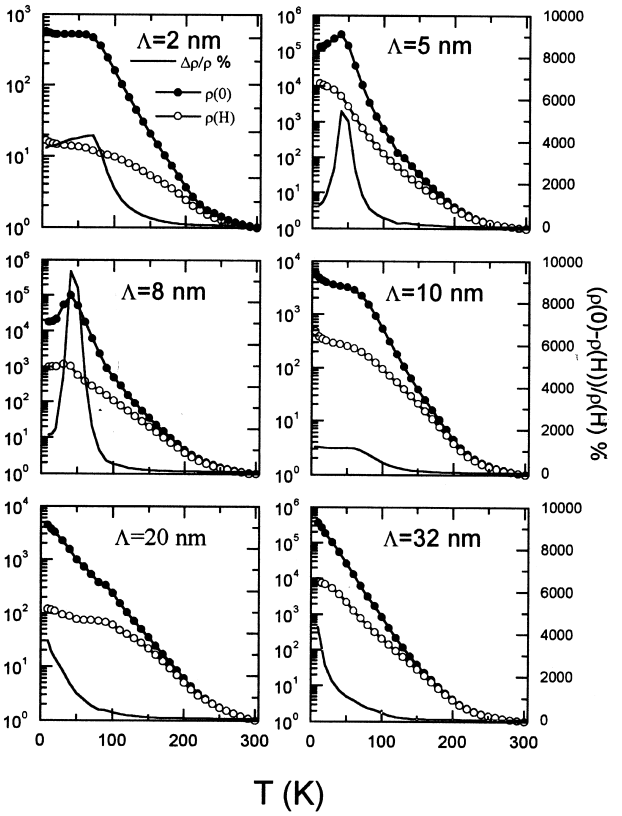

Fig. 6. Resistivity, normalized to the 300 K value, as a function of temperature, measured in 50 kOe (ρ_H) and in zero applied field (ρ_0) for the series of $[FM(\Lambda/2)/AF(\Lambda/2)]_{15}$ multilayers. The CMR ratio $\Delta\rho/\rho_H = [\rho_0 - \rho_H]/\rho_H$ is plotted as a solid line.

few atomic planes near the AF/FM interfaces, defining an active film volume V_{int}. Since T_B results from a thermally activated process, following an Arrhenius law [23] its value depends on the active volume at the interfaces $T_B V_{int}$ which emerges to be similar in the examined multilayers.

Fig. 5 shows the variation of the normalized resistivity as a function of temperature, measured in 50 kOe (ρ_H) and in zero applied field (ρ_0). The resistivity increases drastically as we cool down from 300 K, spanning almost four orders of magnitude. Also, the CMR ratio becomes maximum in the temperature range below T_B. In Fig. 5 the steep increase of resistivity at low temperatures is in contrast with the decrease of ρ observed in epitaxial FM films [24,25]. This provides further experimental evidence that the insulating behavior [26] of the AF layer is dominant at low-temperatures. This extra contribution in ρ is different for every specimen and modifies the shape of the resultant CMR curves (Fig. 6). Clearly, the multilayers with $\Lambda = 5$ and 8 nm exhibit a peak in the CMR response, indicating a special arrangement of spins at the AF/FM interfaces. Also the characteristic CMR peak, that is usually reported nearby the ferromagnetic T_C of $La_{2/3}Ca_{1/3}MnO_3$ films [27], is not observed in the ρ_0 versus temperature curve. This behavior is in agreement with the magnetothermal measurements (Fig. 5), where it is evident that the most drastic change of the average film magnetization does not occur near the T_C of the individual FM layers but at T_B.

In summary, we have studied the variation of exchange biasing and coercive field as a function of Λ and temperature in $La_{2/3}Ca_{1/3}MnO_3/La_{1/3}Ca_{2/3}MnO_3$ multilayers grown by PLD. The maximum $H_{EB} = 880$ Oe was observed for the sample with $\Lambda = 10$ nm. The exchange biasing mechanism sets-in below a blocking temperature of 70 K and induces: (i) an enhancement of H_C in the FC hysteresis loops, (ii) an increase of the CMR ratio.

References

[1] A.P. Ramirez, J. Phys. Condens. Matter 9, (1997) 8171–8199 and references therein.
[2] Yu Lu, et al., Phys. Rev. B 54 (1996) R8357.
[3] J.S. Sun, et al., Appl. Phys. Lett. 69 (1996) 3226.
[4] N.D. Mathur, et al., Nature 387 (1997) 266.
[5] Steenbeck, et al., Appl. Phys. Lett. 73 (1998) 2506.
[6] C. Srinitiwarawong, et al., Appl. Phys. Lett. 73 (1998) 1140.
[7] J.M.D. Coey, J. Appl. Phys. 85 (1999) 5576.
[8] K. Ghosh, et al., Appl. Phys. Lett. 73 (1998) 689.
[9] M. Sahana, et al., J. Appl. Phys. 85 (1999) 1058.
[10] M. Ziese, et al., Phys. Rev. B 57 (1998) 2963.
[11] R. Cheng, et al., Appl. Phys. Lett. 72 (1998) 2475.
[12] W.H. Meiklejohn, C.P. Bean, Phys. Rev. 105 (1957) 904.
[13] C. Tsang, N. Heiman, K. Lee, J. Appl. Phys. 52 (1981) 2471.
[14] R. Jungblut, et al., J. Appl. Phys. 75 (1994) 6659.
[15] P.J. van der Zaag, et al., J. Appl. Phys. 79 (1996) 5103.
[16] K. Takano, et al., Phys. Rev. Lett. 79 (1997) 1130.
[17] T. Ambrose, R.L. Sommer, C.L. Chien, Phys. Rev. B 56 (1997) 83.
[18] Y. Ijiri, J.A. Bochers, et al., Phys. Rev. Lett. 80 (1998) 608.
[19] J. Nogues, et al., Appl. Phys. Lett. 68 (1998) 3186.
[20] E.F. Fullerton, Phys. Rev. B 45 (1992) 9292.
[21] J. Mattson, J. Appl. Phys. 67 (1990) 2873.
[22] R.A. Rao, et al., Appl. Phys. Lett. 73 (1998) 3294.
[23] B.D. Cullity, Introduction to Magnetic Materials, Addison-Wesley, Reading, MA, 1972.
[24] I. Panagiotopoulos, et al., Mater. Sci. Eng. B 53 (1998) 272.
[25] Q. Huang, et al., Phys. Rev. B 58 (1998) 2684.
[26] M.T. Fernandez-Diaz, Phys. Rev. B 58 (1999) 1277.
[27] P. Schluffer, et al., Phys. Rev. Lett. 75 (1995) 3336.
[28] W.H. Meiklejohn, C.P. Bean, Phys. Rev. 102 (1956) 1413.
[29] C. Tsang, N. Heiman, K. Lee, J. Appl. Phys. 53 (1982) 2605.